



Preparation, characterisation and sensing application of inkjet-printed nanostructured TiO₂ photoanode

Min Yang, Lihong Li, Shanqing Zhang*, Guiying Li, Huijun Zhao

Environmental Futures Centre, and Griffith School of Environment, Gold Coast Campus, Griffith University, QLD 4222, Australia

ARTICLE INFO

Article history:

Received 13 January 2010

Received in revised form 12 March 2010

Accepted 12 March 2010

Available online 3 April 2010

Keywords:

Inkjet printing

Photoelectrochemical

Sensors

TiO₂

ABSTRACT

Inkjet printing technique is proposed for the fabrication of titanium dioxide (TiO₂) photoanodes with a synthetic colloidal TiO₂ ink. The resultant electrodes were characterised using materials characterisation methods (such as scanning electron microscope, X-ray diffraction and UV–vis spectrophotometer) as well as photoelectrochemical means. The preliminary results indicate that the nanostructure of the original TiO₂ particles is well maintained in the printing process, and the thickness and uniformity of the TiO₂ thin film can be well controlled by the simple printing technique. Combined with photoelectrochemical means, the inkjet-printed TiO₂ photoanode is capable of oxidising organic compounds in aqueous solution, including weak organic adsorbates (e.g., glucose, phenol) and strong organic adsorbates (e.g., potassium hydrogen phthalate (KHP), glutaric acid, malonic acid) indiscriminately in bulk cell. This characteristic is utilized to determine chemical oxygen demand (COD) in aqueous samples. A linear range of 0–120 mg/L of O₂ and a detection limit of 1 mg/L of O₂ were achieved. The photoelectrochemical activity of the printed electrodes was found to be highly reproducible. Inkjet-printing technique can be a versatile method for mass production of TiO₂ photoanodes as sensors.

Crown Copyright © 2010 Published by Elsevier B.V. All rights reserved.

1. Introduction

Since Fujishima and Honda discovered the photocatalytic splitting of water on a TiO₂ electrode under ultraviolet light in 1972 [1], the research of TiO₂ material has attracted tremendous attention from scientists and engineers. Due to the strong oxidation power of TiO₂ semiconductor material under UV illumination, TiO₂ photoanode has been also used in advanced oxidation processes (AOPs) and photoelectrochemical sensing of organic compounds [2]. However, there are still not many practical devices for sensing applications in the market to match the effort and investments attracted from the researchers and developers worldwide. This is partly because of the lack of cost-effective mass production technology that can be used to produce robust and highly reproducible TiO₂ photoanodes.

Various techniques have been employed to immobilize TiO₂ nanoparticles on a substrate, including sol–gel dip-coating [3,4], spin-coating [5,6], sputtering [7,8], spray pyrolysis [9,10], atomic layer deposition [11,12], chemical vapour deposition [13,14] and electrodeposition [15]. Among them, sol–gel dip-coating method was often selected to fabricate TiO₂ nanostructured photoanodes for sensing application, e.g., PeCODTM technology [4], since the dip-coating method is simple, low cost and capable of maintaining the nanostructure of TiO₂. However, in the production of pho-

toanodes, it is found that the photoanodes obtained from the dip-coating technique were quite different from each other in terms of sensitivity and reproducibility. Considerable time and effort is therefore required to calibrate the photoanode individually, the actual cost for the individual photoanode soars dramatically due to this additional cost of the calibration process. Comparing with the dip-coating technique, inkjet printing technique is a potential candidate that can achieve mass production of uniform and reproducible sensors, and eliminate the calibration cost. This technique has been explored extensively as a versatile research tool in materials and devices manipulation [16–18] due to the advantages of high reproducibility, fast production and easy production automation. Recently, Bernacka-Wojcik et al. fabricated dye sensitized TiO₂ photodetectors for DNA biosensors using the inkjet printing technique [19], which demonstrated that this technique was ideal for cost efficient mass production.

In this study, inkjet printing technique was used to immobilize TiO₂ nanoparticulates on the conducting ITO substrates to construct reproducible and uniform sensors. The resultant TiO₂ thin film was characterised using scanning electron microscope (SEM), X-ray diffraction (XRD) and UV–vis spectrophotometer. The suitability of the resultant TiO₂ photoanode for sensing application was investigated using photoelectrochemical bulk cell, detecting a range of organic compounds, such as glucose, phenol, potassium hydrogen phthalate (KHP), glutaric acid and malonic acid, as well as chemical oxygen demand (COD), an important aggregative parameter of organic waste in water quality [20,21].

* Corresponding author. Tel.: +61 7 5552 8155; fax: +61 7 5552 8067.

E-mail address: s.zhang@griffith.edu.au (S. Zhang).

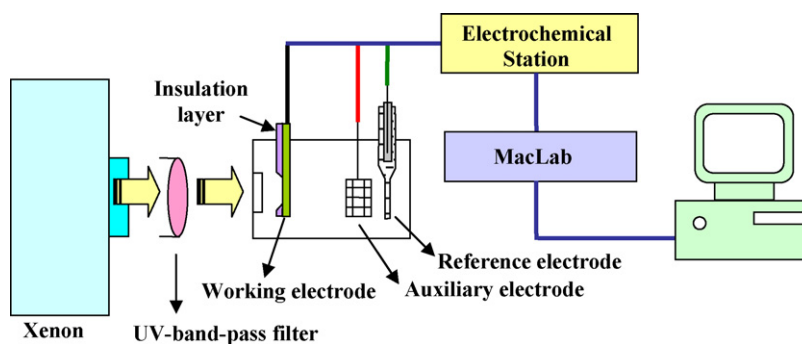


Fig. 1. The setup of the photoelectrochemical bulk cell.

2. Materials and methods

2.1. Chemicals and materials

Indium tin oxide (ITO) conducting glass slides were purchased from Delta Technologies Ltd. (USA). Titanium (IV) butoxide (97%), isopropanol, D-glucose (Merck), potassium hydrogen phthalate (KHP), phenol, glutaric acid, malonic acid, sodium nitrate, nitric acid and carbowax (20 M, Supelco) were used as received. All chemicals were of analytical grade and purchased from Sigma–Aldrich unless otherwise stated. All solutions were prepared using Milli-Q water (Millipore Corp., 18 M Ω cm).

2.2. Preparation of TiO₂ colloid

The TiO₂ colloid was prepared according to our previous work [22]. Aqueous TiO₂ colloid was prepared by the hydrolysis of titanium butoxide [23]. The colloid containing 60 g/L TiO₂ solid was obtained. The TiO₂ colloidal ink was finally formed by dissolving 1.8% (w/w) of carbowax into the above TiO₂ colloid.

2.3. Preparation and characterisation of TiO₂ thin film

Inkjet-printed photoanodes were fabricated using a piezoelectric inkjet printer (Epson R290) while dip-coated photoanodes were prepared using a dip-coater (TL 0.01, Kejing, Shenyang, China). All the photoanodes were calcined at 700 °C in a muffle furnace for 2 h. Transmittance spectra were obtained using UV-1601 spectrophotometer (Shimadzu, Japan). The surface morphology of the inkjet-printed TiO₂ film was characterized by scanning electron microscopy (SEM, JSM 890). The crystalline phase of the TiO₂ thin film was determined by XRD using a diffractometer (Philips PW3020) with Cu K α radiation.

2.4. Photoelectrochemical setup of bulk cell

A three-electrode photoelectrochemical bulk cell (see Fig. 1) was used to investigate the photoelectrocatalytic oxidation of organic compounds. The experiments were performed at room temperature (23 °C). The inkjet-printed TiO₂ electrode was used as the working electrode and placed in an electrode holder with ca. 0.78 cm² left unsealed to be exposed to the solution for illumination and reaction. A saturated Ag/AgCl electrode and a platinum mesh were served as the reference and auxiliary electrodes, respectively. The supporting electrolyte was 0.1 M NaNO₃. A voltammograph (CV-27, BAS) was used to monitor the current under a constant potential and linear scanning potentials. Potential and current signals were recorded by a PC coupled with a MacLab 400 interface (AD Instruments). A 150 W Xenon (HFC-150, TrustTech, Beijing, China) with regulated optical output was used as the UV light source. A

UV-band-pass filter (UG-5, Schott) was installed before the quartz window of the photoelectrochemical cell to prevent the testing solution from being heated up. The UV light intensity illuminated at the electrode surface was 6.6 mW/cm², measured at 365 nm wavelength using a UV irradiance meter (UV-A Instruments of Beijing Normal University).

3. Results and discussion

3.1. Inkjet printing of TiO₂

3.1.1. Selection of printing technology

Most researches on inkjet printing require expensive and specialized inkjet printers, which are not always available in common laboratories. There are two major printing technologies available in the market. One is bubble-jet printing technology (e.g., Canon printers) that involves an ink heating process during the printing process. The other is piezoelectric printing technology (e.g., Epson and HP printers). In this work, Epson R290 printer for office use was chosen due to the following technical features besides its low cost. (a) Printing with the piezoelectric print head does not involve an ink heating process and therefore the printing process is immune from aggregation of the TiO₂ nanoparticles in the ink. The aggregation could destroy the nanostructure of the TiO₂ nanoparticles, affect the uniformity of the printed pattern, and may permanently block the printer nozzles. In fact, this particle aggregation was observed in the bubble-jet printer trials. (b) The Micro Piezo print head technology takes full advantage of high-precision microelectronics to create perfectly spherical ink droplets at sizes as small as 1.5 pL. The printer possesses a very high resolution and therefore it has good control of the printed ink quantity and can achieve high reproducibility. (c) The attached CD-print tray and labelling software make the creation of desired dimension and pattern simple and straightforward. Numerous pieces of substrates (e.g., ITO conducting glass with a thickness up to 2 mm) can be fitted onto the CD-print tray at a time, depending on the size of the substrate. It does not require any modification for either the printer hardware or software to print the photoanodes. (d) The sponge-free internal structures of the ink cartridge are suitable for colloidal ink printing. The ink cartridge can be cleaned and reused easily.

3.1.2. Colloidal TiO₂ ink formulation

TiO₂ concentration is one of the most important parameters for the colloidal TiO₂ ink, and thus it needs to be selected at the first place for effective and smooth printing process. A too high TiO₂ concentration blocks the printer nozzle easily and may lead to the aggregation of TiO₂ nanoparticles, affecting the nanostructure of the resultant photoanode. In contrast, a too low TiO₂ concentration requires too many times of printing for a meaningful loading of the photocatalyst on the conducting ITO substrate. Interestingly, 6% (w/w) of TiO₂, the concentration used as the dip-coating solution

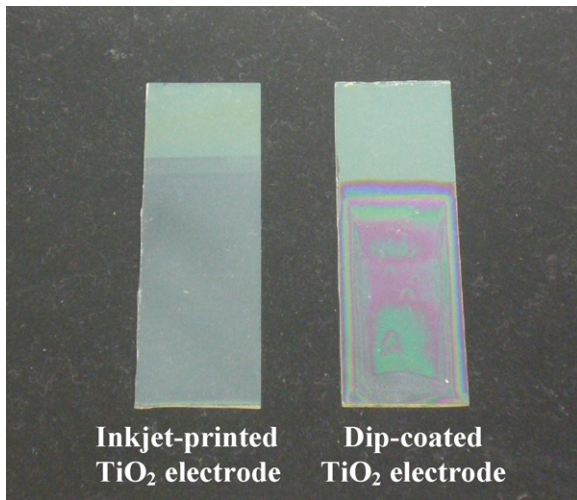


Fig. 2. Images of the inkjet-printed TiO₂ electrode (left) and dip-coated electrode (right).

for TiO₂ photoanodes in our previous work [4] was found to be suitable for inkjet-printing as well.

The physicochemical characteristics of the ink are essential for printing high resolution and well-defined patterns. Among them, viscosity and surface tension are the most crucial in this process [24]. The viscosity of the ink needs to be adjusted in a suitable range. On one hand, it needs to be sufficiently high (i.e., greater than 1 cP) to allow the smooth delivery of the “ink” between the printer head and the cartridge. For example, it was observed that Epson R290 printer could not print the liquid with viscosity of <1 cP, e.g., water. Because of this reason, the routine printer head cleaning is carried out using 5% (w/w) carbowax solution (viscosity 4 cP) instead of pure water. On the other hand, the viscosity should be sufficiently low as the spraying power generated by the piezoelectric membrane is very limited. The suitable viscosity for inkjet printing needs to be below 20 cP [25]. The colloidal TiO₂ ink we used was made of carbowax (1.8%, w/w) and TiO₂ (6%, w/w), and its viscosity was 4 cP which was in the range of the above requirement for this type of inkjet printer (i.e., 1 cP < viscosity < 20 cP). Besides being used for adjusting the viscosity, carbowax also acts as a binder for TiO₂ thin film and pore generator during the subsequent calcination process at 700 °C [26–28].

Surface tension plays an important role on the interaction between the printer nozzle and ink, as well as the spreading of this pico-liter droplet over the substrate surface. Ideally, the surface tension must be high enough to be held in the nozzle without dripping and low enough to allow the droplet spreading over the substrate surface to form a continuous film. In this case, the surface tension of the ink should be between 28 and 350 mN/m² [25]. The surface tension of the TiO₂ ink we used was 56 mN/m², which was in the required range. Consequently, the ink with carbowax (1.8%, w/w) and TiO₂ (6%, w/w) was employed to prepare TiO₂ nanostructured photoanodes for the subsequent investigations using inkjet printing and dip-coating techniques.

3.2. Materials characterisation

The images of a typical inkjet-printed electrode (10 layers) and a dip-coated TiO₂ electrode are shown in Fig. 2. It can be visually observed that the inkjet-printed electrode was more uniform than the dip-coated one, evidenced by the light diffraction patterns on the dip-coated electrode. The formation of the diffraction patterns was due to surface tension attracted the liquid layer to the liquid centre during the drying process after the substrate was

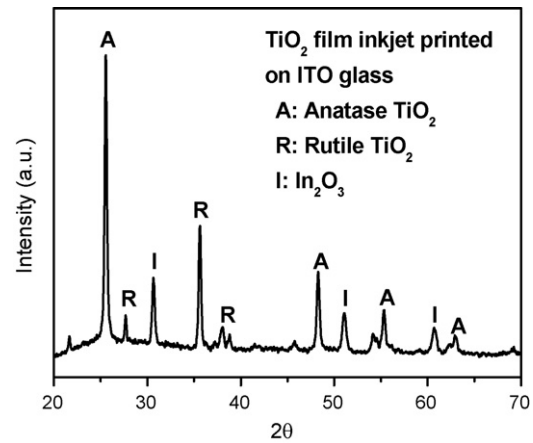


Fig. 3. XRD pattern of the inkjet-printed TiO₂ electrode on ITO substrate calcinated at 700 °C for 2 h.

dipped and withdrawn from the colloidal solution. Consequently, the dip-coated TiO₂ layer was thick at the centre and thin at the edge. In strong comparison, no diffraction pattern was observed on the inkjet-printed electrode because the micro-droplet evaporated rapidly on the electrode surface and the surface tension was of no effect on the drying process.

Fig. 3 shows the XRD pattern of the crystalline phase of the TiO₂ inkjet-printed electrode that has been calcined at 700 °C for 2 h. The film mainly consists of anatase since the characteristic diffraction peaks of anatase at 2θ degrees of 25.56, 48.28 are evident in the sample; while the peaks at 2θ degrees of 27.5 and 35.6 are ascribed to rutile. The crystalline compositions of the TiO₂ electrodes are 92.9% of anatase and 7.1% of rutile.

The UV–vis transmittance spectra of the ITO glass and inkjet-printed TiO₂ electrodes with different number of layers are shown in Fig. 4. It indicates that ITO glass has good transmittance in the visible light and near UV region. With each successive print of TiO₂, the transmittance in the visible light range was not significantly affected due to visible light transparency nature of the TiO₂ film. In contrast, the transmittance in UV range decreased dramatically in range of 300–450 nm due to the introduction of TiO₂ film. Fig. 4 also shows a clear trend that more UV light is absorbed with the increased number of layers (i.e., printing times). This suggests the UV adsorption amount can be controlled by the printing times. It can be also seen from Fig. 4 that 1-layer TiO₂ film can absorb almost all UV light with wavelength of <300 nm, while 10-layer TiO₂ film can absorb nearly all UV light with wavelength of <340 nm.

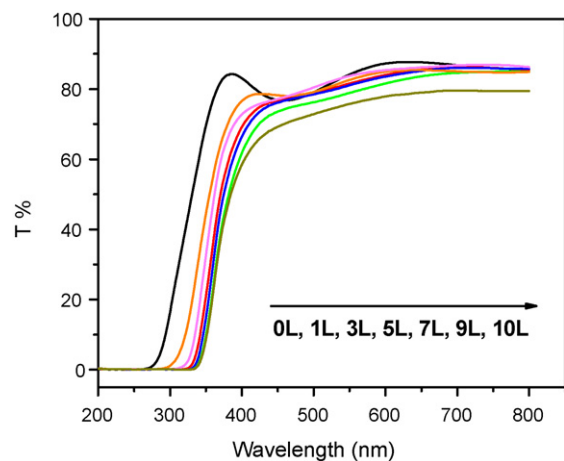


Fig. 4. Transmittance spectra of ITO glass substrate and inkjet-printed TiO₂ electrodes with different layers.

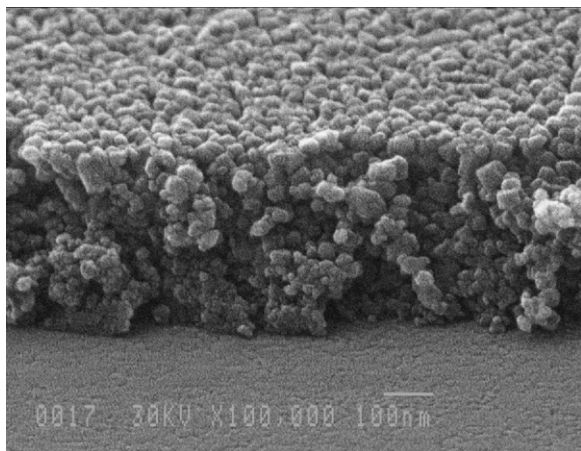


Fig. 5. SEM cross-sectional image of the 10-layer inkjet-printed TiO₂ electrode.

The surface morphology of the film was examined by SEM. The crystalline size within the range of 20–40 nm was observed, similar to the particle size of the dip-coated electrode [29], suggesting the 700 °C high temperature calcination process could lead to aggregation of the primary nanoparticles (ca. 10 nm) of the TiO₂ colloid, which was observed by TEM [29]. The cross-section image indicated the thickness of the 10-layer TiO₂ film was ca. 400 nm (see Fig. 5). More importantly, the image reveals that the inkjet-printed TiO₂ film has a uniform and porous surface and internal structure, which is in line with the observation of Fig. 2. The printed layers merged so well that no gap could be observed between printed TiO₂ layers. This can be attributed to the suitable viscosity and surface tension of the colloidal TiO₂ ink.

3.3. Photoelectrochemical characterisation

The thickness of the TiO₂ thin film plays an important role on the photocatalytic activity [30–32]. The thickness was controlled by the number of printing times in this work. Fig. 6 shows the voltammograms recorded for the inkjet-printed TiO₂ film electrodes with different number of printed layers in an aqueous solution (0.1 M NaNO₃). The measured photocurrent was purely generated from the oxidation of water by the photo holes because there was no other oxidisable substance in the solution. The voltammograms of the inkjet-printed electrodes (i.e., from 1 to 10 layers) shared a similar shape, i.e., the photocurrent initially increased linearly with

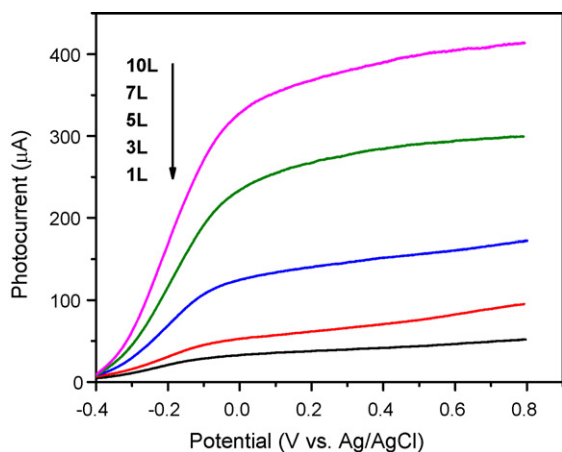


Fig. 6. Voltammograms of the inkjet-printed TiO₂ electrodes with different layers obtained in 0.1 M NaNO₃ solution. Scanning rate: 5 mV/s. Light intensity: 6.6 mW/cm².

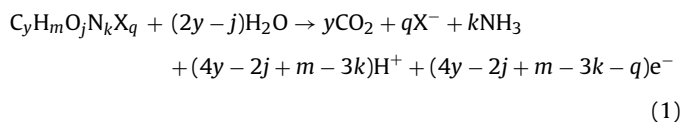
increase of applied potential bias and then levelled off at higher applied potential.

The voltammograms can be explained by the following: photoinduced electron–hole pairs are generated under the illumination of UV light. Separate efficiency of electron–hole pairs determines the photocatalytic oxidation ability. Potential bias is considered to act as a driving force for separation of photoinduced electrons and holes. The electron transfer in the photocatalytic oxidation process involves two major processes. One is the electron transport within the TiO₂ film and the other is the electron injection at the interface (photohole capture). The linear photocurrent responses at lower potential can be attributed to the limitation of free photoelectron transport inside the TiO₂ film, while the saturation indicates that the photohole capture process controls the overall photocatalysis reaction [29,33].

The extent of the saturation current of an electrode can be considered as the photocatalytic oxidation capacity. As shown in Fig. 6, with the increase of the number of layers, the saturation current increased, suggesting the photocatalytic oxidation ability was enhanced. However, when the number of layer increased to over 10, film peeling-off was observed after the calcination process. Therefore, considering the positive effect of the number of printed layers on the photocurrent and the photocatalytic properties, the 10-layer printed TiO₂ electrodes was chosen for the later photoelectrochemical experiments.

3.4. Photoelectrocatalytic oxidation of organic compounds

The general equation for complete mineralization of an organic compound, C_yH_mO_jN_kX_q, on a TiO₂ electrode can be represented by Eq. (1): [4]



where X represents a halogen atom. The electron transfer number (*n*) in the complete mineralisation of the organic compound is equal to 4y – 2j + m – 3k – q. The photocurrent obtained in the oxidation process represents the photoelectrocatalytic activity and effectiveness of oxidation process.

Organic compounds with different functional groups have various adsorptivity to TiO₂ surface [34–36]. They can be classified into weak adsorbates (such as hydroxyl organic compounds, e.g., glucose, phenol, etc.) and strong adsorbates (such as organic compounds containing carboxylic functional group, e.g., phthalic acid, glutaric acid and malonic acid, etc.). Glucose, as a representative of the weak adsorbates, was firstly investigated under an UV illumination intensity of 6.6 mW/cm². As the photocurrent was levelled off at high potential bias (i.e., more positive than +0.0 V), a potential bias of +0.3 V was chosen for subsequent photocatalytic experiments because the recombination of photoinduced electron–hole pairs can be sufficiently suppressed [37]. The photocurrent profiles of different glucose concentrations under a constant potential of +0.3 V are shown in Fig. 7. Without the UV illumination, the dark current was approximately zero for all glucose concentrations, which confirms that the glucose cannot be electrochemically oxidised by the TiO₂ electrode. Upon illumination, the current increased rapidly and then decayed right after the current reached its peak, and subsequently reached steady state.

Fig. 8 shows a set of photocurrent–time profiles obtained in the presence and absence of glucose in the photoelectrochemical bulk cell. The photocurrent for the blank (the dash line), originated purely from the oxidation of water is designated as *i*_{blank}, while the photocurrent resulted from the sample solution containing glucose

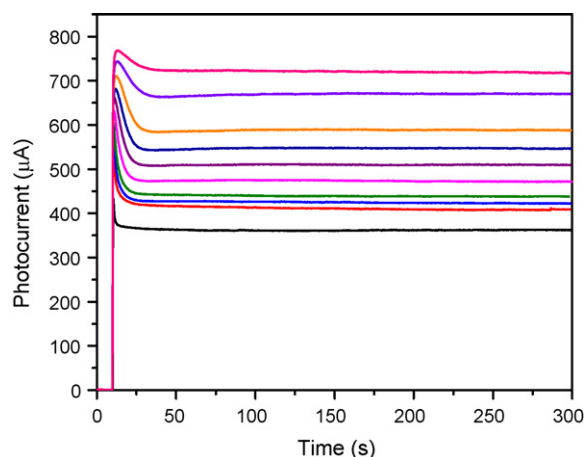


Fig. 7. A set of photocurrent response of a 0.1 M NaNO₃ blank solution and 0.1 M NaNO₃ solution containing different concentrations of glucose. From bottom to top: 0, 100, 150, 200, 300, 400, 500, 600, 800, and 1000 μM glucose. Applied potential: +0.3 V vs. Ag/AgCl. Light intensity: 6.6 mW/cm².

is defined as i_{total} . i_{total} consists of two components, one from the oxidation of water, which is the same as i_{blank} , and the other from photoelectrocatalytic oxidation of organic compound (i.e., glucose). The latter one is named as net current (i_{net}), i.e., the limiting current, originated from the oxidation of organics. i_{net} can be obtained by subtracting i_{blank} from i_{total} (see Eq. (2)).

$$i_{net} = i_{total} - i_{blank} \quad (2)$$

According to Fick's law, the quantitative relationship between the i_{net} and the molar concentration (C_b) of an individual analyte can be written as Eq. (3) [21], where n is the number of electrons transferred for the complete mineralization of an organic compound, A and F refer to electrode geometric area and Faraday constant, respectively, D is the diffusion coefficient of the compound, and δ is the thickness of the Nernst diffusion layer.

$$i_{net} = \frac{nFAD}{\delta} C_b \quad (3)$$

Fig. 9 shows the plot of i_{net} against C_b using the 10-layer printed TiO₂ electrode. Good linear relationships between i_{net} and molar concentrations of all the investigated organic compounds (i.e., KHP, phenol, glucose, glutaric acid, malonic acid).

In our previous work, the net steady state currents originated from the oxidation of organic compounds were found to be directly proportional to COD concentrations [21]. The molar concentration

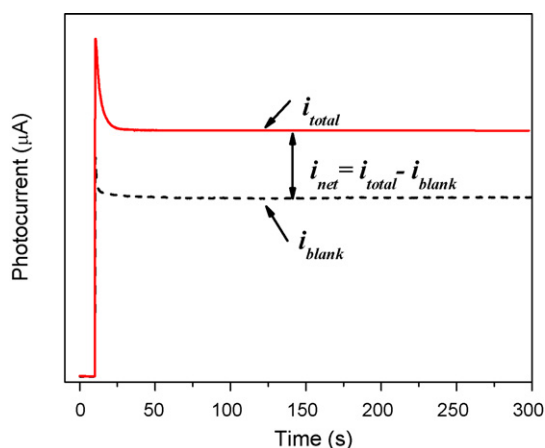


Fig. 8. Determination of the limiting current (i_{net}) by subtracting the blank current (i_{blank}) from the total current (i_{total}).

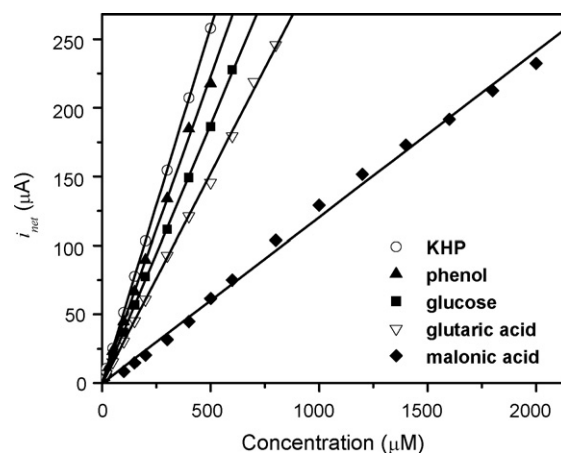


Fig. 9. The relationship between i_{net} and the molar concentrations of different organic compounds.

can be converted into the equivalent COD concentration (mg/L of O₂), using the oxidation number n and the definition of COD [20], i.e., $[\text{COD}] = 8000n \cdot C_b$, we have:

$$i_{net} = \frac{FAD}{\delta} \times \frac{1}{8000} [\text{COD}] \quad (4)$$

We can conclude that i_{net} is directly proportional to COD concentration. i.e.,

$$i_{net} \propto [\text{COD}] \quad (5)$$

Fig. 10 was obtained by plotting i_{net} against the theoretical COD values. Excellent linear relationship between experimental i_{net} and theoretical COD of the investigated organic compounds was obtained. More importantly, the distribution of i_{net} against the COD concentration indicated that these data points shared almost an identical calibration curve when the concentration was below ca. 120 mg/L of O₂. Fig. 10 demonstrates that the 10-layer inkjet-printed TiO₂ electrode can be used as a photoelectrochemical sensor for COD determination. The detection limit and reproducibility of the 10-layer inkjet-printed TiO₂ electrode were also studied. The detection limit of 1 mg/L of O₂ with linear range up to 120 mg/L of O₂ was achieved. A relative standard deviation (RSD) of 3.84% was obtained by performing 25 replicate detections of a sample with a glucose concentration of equivalent to 24 mg/L of O₂.

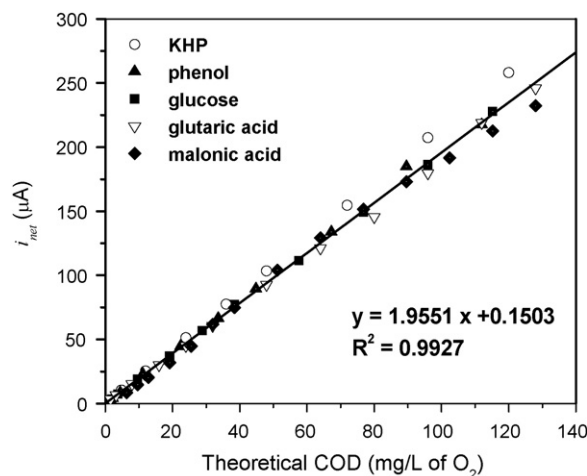


Fig. 10. The relationship between i_{net} and the COD concentrations converted from Fig. 9 using equation $[\text{COD}] = 8000n \cdot C_b$.

The similarity among electrodes was evaluated by measuring the blank and net currents. For 5 dip-coated electrodes from the same batch of TiO₂ colloid, it was observed that their photoelectrochemical responses were significantly different from each other. RSD of 6.90% and 7.29% were obtained from the measurements of the blank currents and the total currents of 24 mg/L of O₂ of glucose, respectively. This problem was overcome by the inkjet printing technique. The difference in the photoelectrochemical responses became remarkably smaller among the inkjet-printed electrodes. For example, for 5 10-layer inkjet-printed electrodes from the same TiO₂ ink, RSD of 3.56%, 3.11% were achieved for the measurements of the blank currents and the total currents of 24 mg/L of O₂ of glucose, respectively. This suggests that the electrodes prepared by the inkjet printing technique are more similar to each other than those by dip-coating technique and the inkjet printing technique is a better technology for mass production of the TiO₂ photocatalytic sensors.

4. Conclusion

Reproducible TiO₂ photoanodes for sensing of organic compounds are prepared using the inkjet printing technique. The photoanodes are capable of photoelectrochemically oxidising various organics (e.g., KHP, phenol, glucose, glutaric acid and malonic acid). The linear relationship between the net photocurrent and the concentration of organics demonstrates the promising potential of the inkjet-printed electrode for sensing application. When it was applied as a sensor for determination of COD, a linear range of 0–120 mg/L of O₂ and a detection limit of 1 mg/L of O₂ were achieved. Moreover, compared with the dip-coated electrodes, the reproducibility of the sensing performances among inkjet-printed electrodes was improved. This improvement helps the inkjet printing technique become a simple, low cost, and versatile technique for mass production of TiO₂ photoanodes.

Acknowledgements

The authors acknowledge the financial support of the ARC discovery and ARC linkage grant from Australian Research Council.

References

- [1] A. Fujishima, K. Honda, Electrochemical photolysis of water at a semiconductor electrode, *Nature* 238 (1972) 37–38.
- [2] X. Chen, S.S. Mao, Titanium dioxide nanomaterials: synthesis, properties, modifications, and applications, *Chem. Rev.* 107 (2007) 2891–2959.
- [3] J. Yu, X. Zhao, Q. Zhao, Photocatalytic activity of nanometer TiO₂ thin films prepared by the sol–gel method, *Mater. Chem. Phys.* 69 (2001) 25–29.
- [4] H.J. Zhao, D.L. Jiang, S.Q. Zhang, K. Catterall, R. John, Development of a direct photoelectrochemical method for determination of chemical oxygen demand, *Anal. Chem.* 76 (2004) 155–160.
- [5] J. Kasanen, M. Suvanto, T.T. Pakkanen, Self-cleaning, titanium dioxide based, multilayer coating fabricated on polymer and glass surfaces, *J. Appl. Polym. Sci.* 111 (2009) 2597–2606.
- [6] T. Watanabe, A. Nakajima, R. Wang, M. Minabe, S. Koizumi, A. Fujishima, K. Hashimoto, Photocatalytic activity and photoinduced hydrophilicity of titanium dioxide coated glass, *Thin Solid Films* 351 (1999) 260–263.
- [7] L. Sirghi, T. Aoki, Y. Hatanaka, Hydrophilicity of TiO₂ thin films obtained by radio frequency magnetron sputtering deposition, *Thin Solid Films* 422 (2002) 55–61.
- [8] L. Sirghi, Y. Hatanaka, Hydrophilicity of amorphous TiO₂ ultra-thin films, *Surf. Sci.* 530 (2003) L323–L327.
- [9] A. Conde-Gallardo, M. Guerrero, N. Castillo, A.B. Soto, R. Fragoso, J.G. Cabañas-Moreno, TiO₂ anatase thin films deposited by spray pyrolysis of an aerosol of titanium diisopropoxide, *Thin Solid Films* 473 (2005) 68–73.
- [10] M.O. Abou-Helal, W.T. Seeber, Preparation of TiO₂ thin films by spray pyrolysis to be used as a photocatalyst, *Appl. Surf. Sci.* 195 (2002) 53–62.
- [11] J. Aarik, A. Aidla, H. Mändar, T. Uustare, Atomic layer deposition of titanium dioxide from TiCl₄ and H₂O: investigation of growth mechanism, *Appl. Surf. Sci.* 172 (2001) 148–158.
- [12] J. Aarik, A. Aidla, T. Uustare, M. Ritala, M. Leskelä, Titanium isopropoxide as a precursor for atomic layer deposition: characterization of titanium dioxide growth process, *Appl. Surf. Sci.* 161 (2000) 385–395.

- [13] A. Mills, N. Elliott, I.P. Parkin, S.A. O'Neill, R.J. Clark, Novel TiO₂ CVD films for semiconductor photocatalysis, *J. Photochem. Photobiol. A: Chem.* 151 (2002) 171–179.
- [14] V.G. Bessergenev, R.J.F. Pereira, M.C. Mateus, I.V. Khmelinskii, D.A. Vasconcelos, R. Nicula, E. Burkel, A.M. Botelho do Rego, A.I. Saprykin, Study of physical and photocatalytic properties of titanium dioxide thin films prepared from complex precursors by chemical vapour deposition, *Thin Solid Films* 503 (2006) 29–39.
- [15] S. Karuppachamy, J.M. Jeong, D.P. Amalnerkar, H. Minoura, Photoinduced hydrophilicity of titanium dioxide thin films prepared by cathodic electrodeposition, *Vacuum* 80 (2006) 494–498.
- [16] K. Kordas, T. Mustonen, G. Toth, H. Jantunen, M. Lajunen, C. Soldano, S. Talapatra, S. Kar, R. Vajtai, P.M. Ajayan, Inkjet printing of electrically conductive patterns of carbon nanotubes, *Small* 2 (2006) 1021–1025.
- [17] H. Sirringhaus, T. Kawase, R.H. Friend, T. Shimoda, M. Inbasekaran, W. Wu, E.P. Woo, High-resolution inkjet printing of all-polymer transistor circuits, *Science* 290 (2000) 2123–2126.
- [18] E. Tekin, P.J. Smith, S. Hoepfner, A.M.J. van den Berg, A.S. Susa, A.L. Rogach, J. Feldmann, U.S. Schubert, Inkjet printing of luminescent CdTe nanocrystal–polymer composites, *Adv. Funct. Mater.* 17 (2007) 23–28.
- [19] I. Bernacka-Wojcik, R. Senadeera, P.J. Wojcik, L.B. Silva, G. Doria, P. Baptista, H. Aguas, E. Fortunato, R. Martins, Inkjet printing and “doctor blade” TiO₂ photodetectors for DNA biosensors, *Biosens. Bioelectron.* 25 (2010) 1229–1234.
- [20] American Public Health Association, American Water Works Association, Water Environment Federation, Standard Methods for the Examination of Water and Wastewater, Apha-Awwa-Wef, Washington, DC, 1995.
- [21] S. Zhang, L. Li, H. Zhao, A portable photoelectrochemical probe for rapid determination of chemical oxygen demand in wastewaters, *Environ. Sci. Technol.* 43 (2009) 7810–7815.
- [22] D. Jiang, H. Zhao, S. Zhang, R. John, Characterization of photoelectrocatalytic processes at nanoporous TiO₂ film electrodes: photocatalytic oxidation of glucose, *J. Phys. Chem. B* 107 (2003) 12774–12780.
- [23] M.K. Nazeeruddin, A. Kay, I. Rodicio, R. Humphry-Baker, E. Mueller, P. Liska, N. Vlachopoulos, M. Graetzel, Conversion of light to electricity by *cis*-X₂Bis(2,2′-bipyridyl)-4,4′-dicarboxylate)ruthenium(II) charge-transfer sensitizers (X = Cl⁻, Br⁻, I⁻, CN⁻, and SCN⁻) on nanocrystalline titanium dioxide electrodes, *J. Am. Chem. Soc.* 115 (1993) 6382–6390.
- [24] P. Calvert, Inkjet printing for materials and devices, *Chem. Mater.* 13 (2001) 3299–3305.
- [25] B.J. de Gans, P.C. Duineveld, U.S. Schubert, Inkjet printing of polymers: state of the art and future developments, *Adv. Mater.* 16 (2004) 203–213.
- [26] H.J. Zhao, D.L. Jiang, S.Q. Zhang, W. Wen, Photoelectrocatalytic oxidation of organic compounds at nanoporous TiO₂ electrodes in a thin-layer photoelectrochemical cell, *J. Catal.* 250 (2007) 102–109.
- [27] B. Guo, Z. Liu, L. Hong, H. Jiang, Sol gel derived photocatalytic porous TiO₂ thin films, *Surf. Coat. Technol.* 198 (2005) 24–29.
- [28] T. Miki, K. Nishizawa, K. Suzuki, K. Kato, Preparation of thick TiO₂ film with large surface area using aqueous sol with poly(ethylene glycol), *J. Mater. Sci.* 39 (2004) 699–701.
- [29] D.L. Jiang, S.Q. Zhang, H.J. Zhao, Photocatalytic degradation characteristics of different organic compounds at TiO₂ nanoporous film electrodes with mixed anatase/rutile phases, *Environ. Sci. Technol.* 41 (2007) 303–308.
- [30] Z. Yi, C. Guofeng, W. Ma, W. Wei, Effect of external bias voltage and coating thickness on the photocatalytic activity of thermal sprayed TiO₂ coating, *Prog. Org. Coat.* 61 (2008) 321–325.
- [31] J. Yu, X. Zhao, Q. Zhao, Effect of film thickness on the grain size and photocatalytic activity of the sol–gel derived nanometer TiO₂ thin films, *J. Mater. Sci. Lett.* 19 (2000) 1015–1017.
- [32] S.-C. Jung, S.-J. Kim, N. Imaishi, Y.-I. Cho, Effect of TiO₂ thin film thickness and specific surface area by low-pressure metal–organic chemical vapor deposition on photocatalytic activities, *Appl. Catal. B* 55 (2005) 253–257.
- [33] D.L. Jiang, H.J. Zhao, S.Q. Zhang, R. John, G.D. Will, Photoelectrochemical measurement of phthalic acid adsorption on porous TiO₂ film electrodes, *J. Photochem. Photobiol. A: Chem.* 156 (2003) 201–206.
- [34] J.M. Pettibone, D.M. Cwiertny, M. Scherer, V.H. Grassian, Adsorption of organic acids on TiO₂ nanoparticles: effects of pH, nanoparticle size, and nanoparticle aggregation, *Langmuir* 24 (2008) 6659–6667.
- [35] A.G. Young, A.J. McQuillan, Adsorption/desorption kinetics from ATR-IR spectroscopy. Aqueous oxalic acid on anatase TiO₂, *Langmuir* 25 (2009) 3538–3548.
- [36] S. Koppen, W. Langel, Adsorption of small organic molecules on anatase and rutile surfaces: a theoretical study, *Phys. Chem. Chem. Phys.* 10 (2008) 1907–1915.
- [37] S. Zhang, L. Li, H. Zhao, G. Li, A portable miniature UV-LED-based photoelectrochemical system for determination of chemical oxygen demand in wastewater, *Sens. Actuators B* 141 (2009) 634–640.

Biographies

Dr. Min Yang obtained her PhD degree in physical chemistry in 2007 from Jilin University, China. She worked as a research fellow in Griffith School of Environment at Griffith University, Australia in 2007–2008. Now she is a postdoc research fellow in Erlangen-Nuremberg University, Germany. Her main research interests include synthesis and characterization of functional semiconductor nanomaterials for photoelectrochemical application, such as photoelectric sensor, photocatalysis, electrochromism and dye-sensitized solar cells.

Ms. Lihong Li was graduated with BSc from Jinan University, China in 2004, and MSc from Zhongshan University, China in 2006. Since 2007, she has been studying her PhD degree in Griffith School of Environment at Griffith University, Australia. Her research focuses on development and optimization of the photoelectrocatalytic system for determination of chemical oxygen demand and organic compounds.

Dr. Shanqing Zhang obtained his PhD degree in analytical chemistry in 2001 at Griffith University, Australia. Since then, he has worked as a research fellow during 2001–2006, senior research fellow during 2007–2008, and Australia Research Council Future Fellow for 2009–2014. Dr. Zhang has been involved in the development of numerous new technologies for water quality monitoring, including COD, BOD, nutrients, and intelligent remote sensing system. He is currently a senior lecturer in water science at Griffith School of Environment, Griffith University, Australia. His research areas also include synthesis and characterization of functional nano-materials for sensing application.

Ms. Guiying Li received her BSc and MSc degree from Nanjing Agriculture University, China in 1996 and Northwest Normal University, China in 2002, respectively.

She is currently completing her PhD degree at Griffith School of Environment, Griffith University, Australia, under the direction of Prof. Huijun Zhao, and Dr. Shanqing Zhang. She is working as an associate professor in Guangzhou Institute of Geochemistry, Chinese Academy of Science. Her research includes photocatalytic and photoelectrocatalytic degradation of organic and biological pollutants in wastewaters.

Prof. Huijun Zhao received his BSc in chemistry in 1982 and MSc in electrochemistry in 1986 from the Northeastern University, China. He completed his PhD in 1993 at the University of Wollongong, Australia, under the supervision of Professor Gordon Wallace. He was a research fellow at the University of Wollongong and the University of Western Sydney from 1993 to 1997, and took a lecturer position in Griffith University in 1997, and was subsequently promoted to professor and the Chair of Analytical Laboratory in 2005. He currently focuses his research on nanostructured materials, photocatalysis and environmental monitoring technology/instrument development.